

Enhanced ferroelectric properties of Pb (Zr 0.53 Ti 0.47) O 3 thin films on SrRuO 3 / Ru/SiO 2 / Si substrates

Y. K. Wang, T. Y. Tseng, and Pang Lin

Citation: [Applied Physics Letters](#) **80**, 3790 (2002); doi: 10.1063/1.1480099

View online: <http://dx.doi.org/10.1063/1.1480099>

View Table of Contents: <http://scitation.aip.org/content/aip/journal/apl/80/20?ver=pdfcov>

Published by the [AIP Publishing](#)

Articles you may be interested in

[Huge Anisotropic Magnetoresistance In Epitaxial Sm 0.53 Sr 0.47 MnO 3 Thin Films](#)

AIP Conf. Proc. **1349**, 703 (2011); 10.1063/1.3606052

[Ferroelectric phase transition in Pb 0.92 Gd 0.08 \(Zr 0.53 Ti 0.47 \) 0.98 O 3 nanoceramic synthesized by high-energy ball milling](#)

J. Appl. Phys. **94**, 6091 (2003); 10.1063/1.1618915

[Ferroelectric BaPbO 3 / PbZr 0.53 Ti 0.47 / BaPbO 3 heterostructures](#)

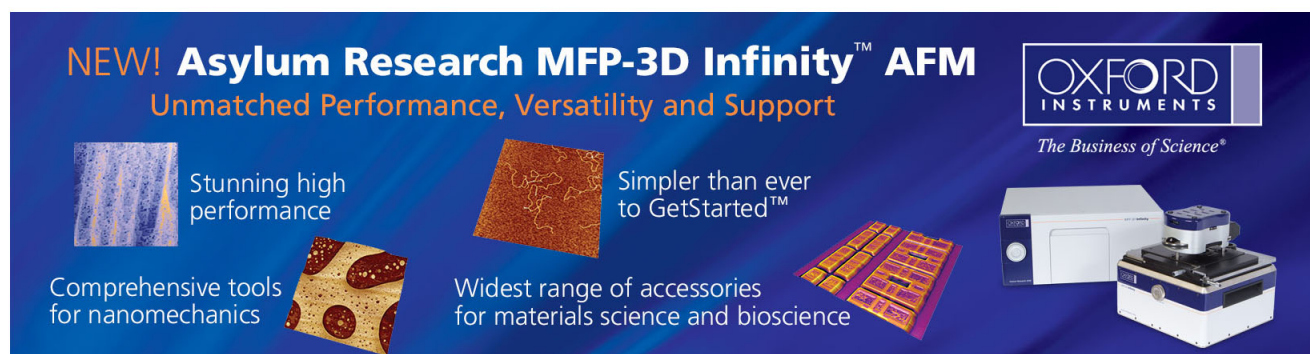
Appl. Phys. Lett. **81**, 3624 (2002); 10.1063/1.1520332

[Lattice strain and lattice expansion of the SrRuO 3 layers in SrRuO 3 / PbZr 0.52 Ti 0.48 O 3 / SrRuO 3 multilayer thin films](#)

J. Appl. Phys. **92**, 101 (2002); 10.1063/1.1483369

[Asymmetry in the hysteresis loop of Pb\(Zr 0.53 Ti 0.47 \) O 3 /SiO 2 /Si structures](#)

J. Appl. Phys. **86**, 4467 (1999); 10.1063/1.371388



NEW! Asylum Research MFP-3D Infinity™ AFM
Unmatched Performance, Versatility and Support


OXFORD INSTRUMENTS
The Business of Science®

Stunning high performance

Simpler than ever to GetStarted™

Comprehensive tools for nanomechanics

Widest range of accessories for materials science and bioscience



Enhanced ferroelectric properties of $\text{Pb}(\text{Zr}_{0.53}\text{Ti}_{0.47})\text{O}_3$ thin films on $\text{SrRuO}_3/\text{Ru}/\text{SiO}_2/\text{Si}$ substrates

Y. K. Wang and T. Y. Tseng^{a)}

Department of Electronics Engineering and Institute of Electronics, National Chiao Tung University, Hsinchu 30050, Taiwan, Republic of China

Pang Lin

Institute of Materials Science and Engineering, National Chiao Tung University, Hsinchu 30049, Taiwan, Republic of China

(Received 12 November 2001; accepted for publication 19 March 2002)

Highly (110)-oriented $\text{Pb}(\text{Zr}_{0.53}\text{Ti}_{0.47})\text{O}_3$ (PZT) films were deposited on SrRuO_3 (SRO)/ $\text{Ru}/\text{SiO}_2/\text{Si}$ substrates using a sol-gel method, in which SrRuO_3 films were deposited at various substrate temperatures. The crystallinity of the PZT films was improved after the annealing process. The leakage current, dielectric constant, and polarization versus electric-field characteristics of PZT films were strongly dependent on the annealing and deposition temperatures of the SRO films. The 650 °C annealed PZT film grown on SRO has a leakage current of 9×10^{-7} A/cm² at an applied field of 500 kV/cm, dielectric constant of 1306, remanent polarization (P_r) of 40.1 $\mu\text{C}/\text{cm}^2$ and coercive field (E_c) of 78.5 kV/cm at an applied voltage of 5 V. The PZT films indicated fatigue-free characteristics up to $\sim 1.0 \times 10^{12}$ switching cycles under 5 V bipolar pulse. © 2002 American Institute of Physics. [DOI: 10.1063/1.1480099]

Ferroelectric thin films of $\text{Pb}(\text{Zr}_x\text{Ti}_{1-x})\text{O}_3$ (PZT) have attracted attention for their applications on ferroelectric random access memory. However, previous reports have indicated that the use of a metal electrode with PZT thin films has serious fatigue problems at a relatively short number of switching cycles because of interface defects such as oxygen vacancies existing between PZT and the metal electrode.¹ Conductive metallic oxide electrodes such as RuO_2 ,² IrO_2 ,³ $(\text{La}_{0.5}\text{Sr}_{0.5})\text{CoO}_3$,⁴ BaRuO_3 ,⁵ and SrRuO_3 (Ref. 6) (SRO) were found to be effective in improving the fatigue properties of PZT film capacitors. Oxide electrodes can act as sinks for oxygen vacancies to suppress polarization fatigue for long switching cycles. On the other hand, the selection of electrode material will determine the microstructure and properties of ferroelectric thin films. The formation of lattice- and chemistry-matched heterostructures of PZT films can be expected with perovskite oxide electrodes because of their similarity in lattice parameter and chemical behavior. This heterostructure usually enhances the ferroelectric characteristics of PZT films.⁷ However, it is very difficult to deposit preferentially oriented PZT and SRO films on silicon substrates, and most studies of epitaxial PZT films on SRO were deposited on SrTiO_3 substrates.⁸⁻¹⁰

In this study, we report on the preparation and properties of highly (110) oriented $\text{Pb}(\text{Zr}_{0.53}\text{Ti}_{0.47})\text{O}_3$ thin films on conducting, highly (110)-preferentially oriented SRO bottom electrodes on silicon substrates.

SRO thin films were deposited on $\text{Ru}/\text{SiO}_2(100\text{ nm})/\text{Si}(100)$ substrates at various temperatures by radio-frequency (rf) magnetron sputtering, using a target made of packed SrRuO_3 powders. The PZT films with a thickness of 200 nm were grown by a sol-gel method, and

annealing was performed in a tube furnace at various temperatures under O_2 atmosphere. The SRO top electrodes with an area of 4.9×10^{-5} cm² were sputter deposited onto the PZT films at room temperature, and then thermally treated at 400 °C for 10 min to reduce interface defects during sputtering. The crystalline properties of the films were examined by x-ray diffraction (XRD, Siemens D5000) with $\text{Cu } K\alpha$ radiation. The surface morphology and microstructure were observed by using atomic-force microscopy (AFM, Digital Instruments Nanoscope III) and scanning electron microscopy (SEM, Hitachi S-4700). The capacitance-voltage ($C-V$)

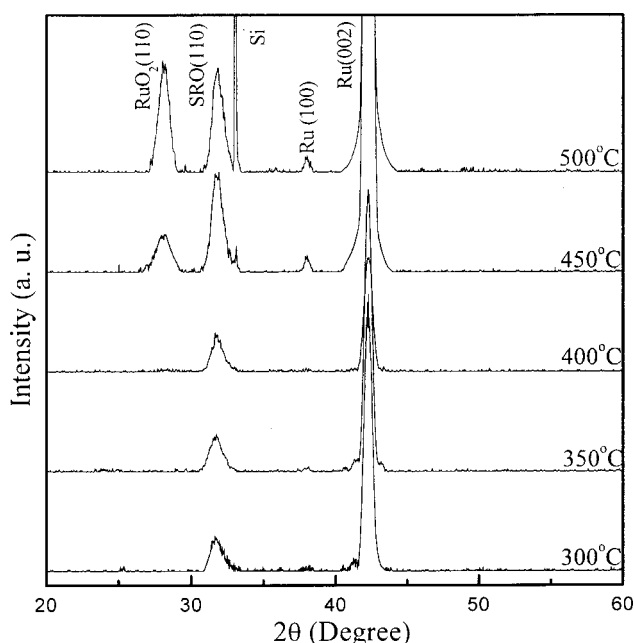


FIG. 1. XRD patterns of SRO films deposited on $\text{Ru}/\text{SiO}_2/\text{Si}$ substrates at various temperatures indicated.

^{a)}Electronic mail: tseng@cc.nctu.edu.tw

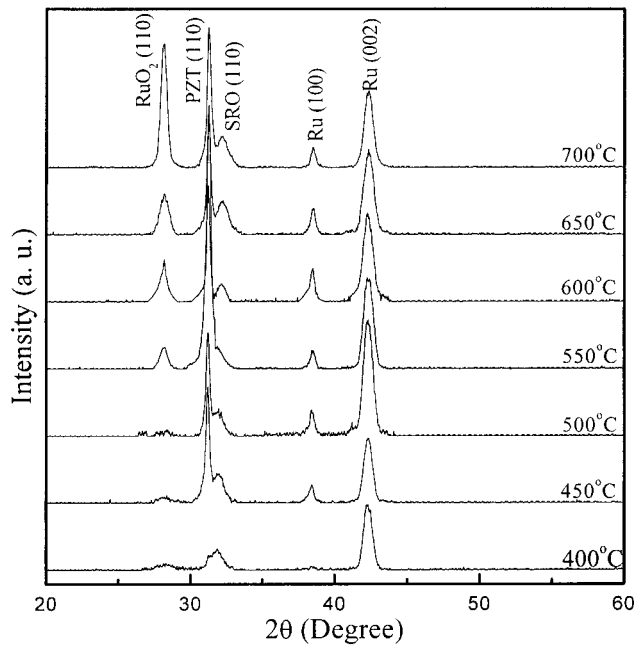


FIG. 2. XRD patterns of PZT films deposited on 450 °C-grown SRO/Ru/SiO₂/Si substrates annealed at various temperatures indicated.

characteristics were measured with an impedance-gain phase analyzer [Hewlett-Packard (HP) 4194A] at 100 kHz. The current–voltage (*I*–*V*) measurements were performed by using a semiconductor parameter analyzer (HP4156B). The ferroelectric properties of the films were measured at 100 kHz using a RT66A ferroelectric tester (Radiant Technologies, Inc.).

Figure 1 shows the XRD patterns of SRO films on Ru/SiO₂/Si substrates deposited at various temperatures. The deposited SRO films exhibit a highly (110)-preferred orientation on the Ru(002) films even if the deposition temperature is as low as at 300 °C. The increase in SRO(110) peak intensity with an increase of temperature implies an improved crystallinity occurred in the films deposited at higher temperature. We found that the RuO₂(110) peak appeared in 450 °C deposited film owing to oxidation reaction at the interface during deposition, and an additional Ru(100) peak also appeared in the meantime. The XRD patterns of PZT films deposited on 450 °C-grown SRO/Ru/SiO₂/Si substrates and annealed at various temperatures are shown in Fig. 2. A strong (110)-preferred orientation appears in the PZT films annealed at 450 °C, and this preferred orientation is enhanced with increasing annealing temperature up to 700 °C. We found in x-ray analysis (not shown here) that the PZT(100) peak also appeared when 300–400 °C-grown SRO electrodes were used. The PZT films deposited at 300 °C on SRO showed an enhanced (100) peak as the annealing temperature increased; however, PZT films deposited at 350 and

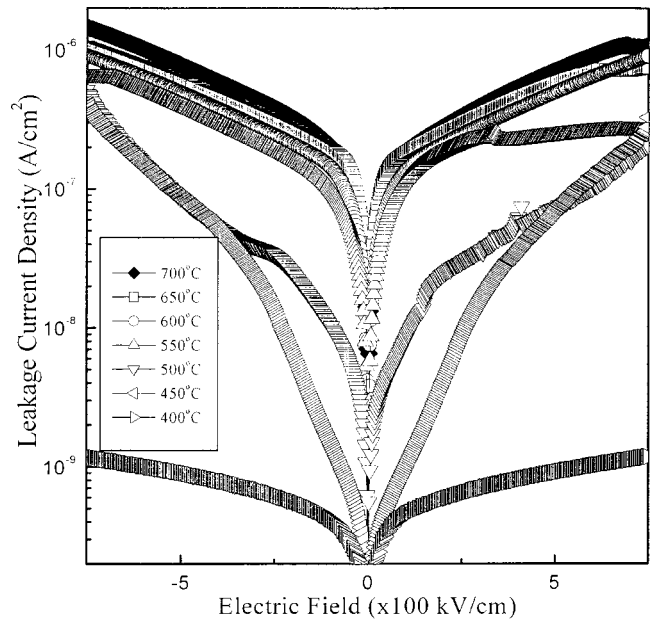


FIG. 3. *I*–*V* characteristics of PZT thin films deposited on 450 °C-grown SRO/Ru/SiO₂/Si substrates and afterward annealed at various temperatures indicated.

400 °C showed no change in the (100) peak intensity as a function of temperature.

The dielectric constant and loss tangent of the PZT films annealed at various temperatures are listed in Table I. The dielectric constant and loss tangent increase with an increase in temperature, which have the highest values of 1541 and 0.137, respectively, for 700 °C-annealed films. Such a high dielectric constant may be attributed to better crystallinity, grain size, and the presence of a thin strain layer between PZT and SRO leading to increased polarization in highly oriented 700 °C-annealed films. Figure 3 shows the leakage current density of PZT films deposited on 450 °C-grown SRO/Ru/SiO₂/Si substrates. The symmetry of the curves indicates the same barrier height for both top and bottom electrodes. The leakage current density for 400 °C-annealed PZT has a small value of less than 10^{–9} A/cm² because of the poor crystallization, whereas the 650 °C-annealed PZT has a leakage current of 9 × 10^{–7} A/cm² at an applied field of 500 kV/cm. It shows that the leakage current increases at high annealing temperature, which is consistent with the result of the loss tangent. This increase may be attributed to the grain growth at high temperature, supplying short-circuit paths when the bias is applied. The grain growth accompanied with the annealing temperature is confirmed by using AFM and SEM observations, as shown in Figs. 4(a)–4(c) and 4(d)–4(f), respectively. It indicates that the film annealed at higher temperature has a larger grain size. In addition, the defect induced by high-temperature annealing, such as lead loss, may also lead to higher leakage current and loss tangent. The

TABLE I. Dielectric constant and loss tangent of PZT thin films deposited on 450 °C-grown SRO and annealed at various temperatures.

Annealing temperature (°C)	400	450	500	550	600	650	700
Dielectric constant	33	165	641	940	1071	1306	1541
Loss tangent	0.011	0.014	0.049	0.105	0.110	0.114	0.137

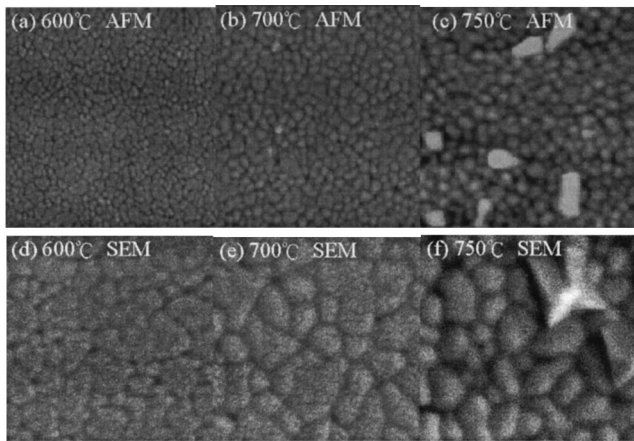


FIG. 4. AFM and SEM images of PZT thin films annealed at various temperatures indicated.

PZT films annealed above 700 °C have a very high leakage current and low breakdown strength. On the basis of AFM and SEM plane-view observations, as indicated in Figs. 4(c) and 4(f), a high surface roughness with protruding grains can be found in 750 °C-annealed PZT film. After applying bias to the top electrode, the high surface roughness of the film could induce the local field that caused the PZT breakdown at low electric field.

The characteristics of fatigue of the 650 °C-annealed PZT films are depicted in Fig. 5, indicating that highly (110)-oriented PZT films deposited on SRO/Ru/SiO₂/Si substrates do not show any deterioration after $\sim 10^{12}$ switching cycles. The polarization–electric-field hysteresis loops of 650 °C-annealed PZT deposited on SRO prepared at various substrate temperatures is also indicated in the inset to Fig. 5. The PZT film deposited on the 350 °C-grown SRO electrode has a higher remanent polarization (P_r) value of 36.6 $\mu\text{C}/\text{cm}^2$, but the P_r value is only 26.6 $\mu\text{C}/\text{cm}^2$ for that deposited on 300 °C-grown SRO. The P_r value of PZT on 300 °C-grown SRO is smaller because this PZT film has a polycrystalline structure; however, highly (110)-preferentially oriented PZT films can be obtained when the bottom electrode SRO was deposited above 350 °C.

In conclusion, we have demonstrated (110) preferentially oriented SRO bottom electrodes deposited on Ru/SiO₂/Si substrates by rf sputtering. PZT thin films deposited on those bottom electrodes also have highly (110)-preferred orientation. The leakage current of PZT films annealed at lower temperatures is smaller than those annealed at higher temperatures, and the reasons for this phenomenon are the grain growth, lead-loss-induced defect, and local field. The dielec-

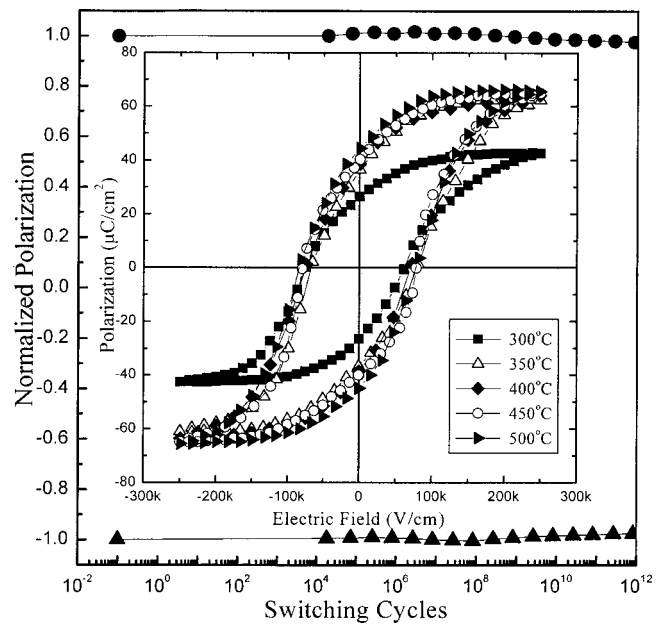


FIG. 5. Fatigue behavior of 650 °C-annealed PZT films deposited on 450 °C-grown SRO/Ru/SiO₂/Si, with a 100 kHz bipolar square-wave peak-to-peak fatigue voltage of 10 V. The inset shows polarization–electric-field hysteresis loops of 650 °C-annealed PZT thin films deposited on SRO bottom electrodes prepared at various temperatures indicated.

tric constant and remanent polarization also increased with an increase of the annealing temperature. PZT films are fatigue free after $\sim 10^{12}$ switching cycles.

This work was supported by the National Science Council R.O.C. under Contract No. NSC 89-2215-E-009-027.

- ¹P. K. Larsen, G. J. M. Dormans, D. J. Taylor, and P. J. van Veldhoven, *J. Appl. Phys.* **76**, 2405 (1994).
- ²S. D. Bernstein, T. Y. Wong, Y. Kisler, and R. W. Tustison, *J. Mater. Res.* **8**, 12 (1993).
- ³T. Nakamura, Y. Nakao, A. Kamisawa, and H. Takasu, *Jpn. J. Appl. Phys., Part 1* **33**, 5207 (1994).
- ⁴R. Ramesh, T. Sands, and V. G. Keramidas, *J. Electron. Mater.* **23**, 19 (1994).
- ⁵C. M. Chu and P. Lin, *Appl. Phys. Lett.* **70**, 249 (1997).
- ⁶C. B. Eom, R. B. VanDover, J. M. Phillips, D. J. Werder, J. H. Marshall, C. H. Chen, R. J. Cava, and R. M. Fleming, *Appl. Phys. Lett.* **63**, 2570 (1993).
- ⁷K. P. Jayadevan and T. Y. Tseng, *Proceedings of ICCE/8*, 5–11 August 2001, Tenerife, Spain (2001), p. 397.
- ⁸J. H. Kim, A. T. Chien, F. F. Lange, and L. Wills, *J. Mater. Res.* **14**, 1190 (1999).
- ⁹C. M. Foster, G. R. Bai, R. Csencsits, J. Vetrone, R. Jammy, L. A. Wills, E. Carr, and Jun Amano, *J. Appl. Phys.* **81**, 2349 (1997).
- ¹⁰K. Nagashima, M. Aratani, and H. Funahubo, *J. Appl. Phys.* **89**, 4517 (2001).